

# Space Object Tracking using a Jump Markov System based $\delta$ -GLMB filter for Space Situational Awareness.

**Diluka Moratuwage**

*Dept. Electrical Engineering,  
Universidad de Chile, Santiago, Chile*

**Martin Adams & Leonardo Cament**

*Dept. Electrical Engineering & Advanced mining Technology Center (AMTC),  
Universidad de Chile, Santiago, Chile*

## ABSTRACT

This paper presents a Bayesian filter based solution to the resident space object (RSO) tracking problem using optical telescopic observations. A multiple Probabilistic Admissible Region (PAR) approach, in which multiple hypotheses are made regarding the region of space where Resident Space Objects (RSOs) can appear, is proposed. These hypotheses provide birth target locations within an adaptive birth based  $\delta$ -Generalized Labeled Multi-Bernoulli ( $\delta$ -GLMB) filter. This is useful since optical based observations do not provide range information. The dynamics of RSOs is modelled using a Jump Markov System (JMS) within the  $\delta$ -GLMB filter. Preliminary results show how telescopic images can be processed to generate suitable data for the tracking of RSOs within a JMS  $\delta$ -GLMB filter.

## 1. INTRODUCTION

The efficient detection, tracking, and cataloging of orbiting RSOs are of paramount importance for improved Space Situational Awareness (SSA). Due to a recent collision, various RSO destructions and an increased number of launches, a higher number of new RSOs now exist. As a result, the demand for modern RSO tracking applications to produce faster, and more efficient detection and tracking capabilities is higher than ever.

Some of the components of the forces acting on RSOs can be considered to vary in a random manner causing their orbits to change over time. Therefore, recursive Bayesian estimation methods have been adopted to detect, track and update the states of RSOs. Under this paradigm, a probability density function of the multi-target state of the set of RSOs entering the field of view (FOV) of a sensor can be propagated in time using captured observations. Traditionally, such solutions initialize the tracks of observed RSOs using a procedure called Initial Orbit Determination (IOD), where an initial estimate of the orbit is refined with a set of further observations using a non-linear optimization approach. Subsequently, the estimated states of the RSOs are propagated by updating a recursive Bayesian filter based on further observations.

Due to the large variance of various orbital parameters, limited FOVs of the sensors and typically small numbers of observations per RSO pass, it is challenging to initialize new tracks and update the existing tracks due to high data association uncertainty when no prior information about the measurements is available. To rectify this problem, the Admissible Region (AR) approach was proposed to limit the candidate RSO orbits to be tracked by selecting either a subset of acceptable range and range rate pairs for optical observations or right ascension rate and declination rate pairs for radar observations [7]. The AR approach was further improved using additional constraints on the orbital properties such as the semi-major axis and eccentricity and then referred to as the Constrained Admissible Region (CAR). This concept is demonstrated in Fig. 1.

The hard constraints of the CAR approach have been replaced with a probabilistic representation, called the Probabilistic Admissible Region (PAR) method, to facilitate orbit initiation in Bayesian tracking methods using optical telescopic observations [3].

Several Bayesian RSO tracking algorithms have been developed using the CAR and PAR approaches, including the recent Random Finite Set (RFS) based methods of Jones et al. [4]. Almost all these solutions model RSOs using

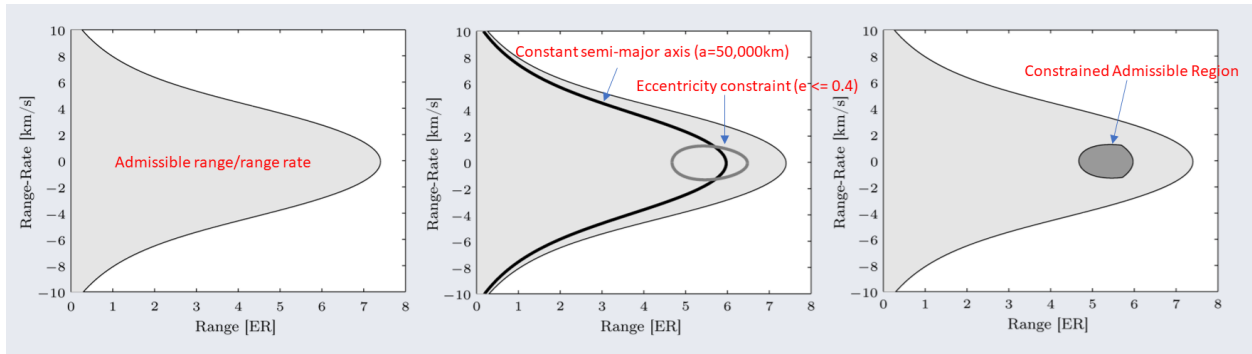


Fig. 1: The Constrained Admissible Region (CAR) approach for initializing target tracks.

a single motion model. This limits the number of trackable orbits to those that satisfy the imposed CAR or PAR constraints. Furthermore, unless prior information about the RSOs being observed is available, a large portion of observations may not be usable in optical observation based tracking solutions. This is demonstrated in Fig. 2. Therefore, in this article, an RFS based RSO tracking algorithm for optical observations is proposed to address these

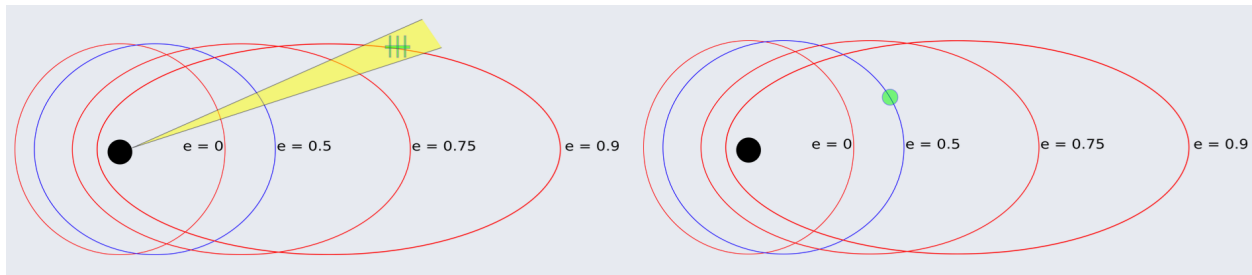


Fig. 2: (Left) Due to birth modelling with a single CAR corresponding to the orbit with eccentricity  $e = 0.5$  (blue ellipse) a target track for the RSO in the orbit with  $e = 0.9$  cannot be initialized. (Right) Only RSOs in the orbit with  $e = 0.5$  (blue ellipse) can be tracked.

limitations using the recently introduced efficient variant of the  $\delta$ -GLMB filter based on the Gibbs sampler [9].

Instead of a single CAR, multiple disjoint CARs are defined, such that orbits ranging from Low Earth Orbit (LEO), Medium Earth Orbit (MEO), Geosynchronous Earth Orbit (GEO), Geosynchronous Transfer Orbit (GTO) to High Earth Orbit (HEO) are classified into a predefined set of CARs depending on their orbital properties such as semi-major axis, eccentricity, altitude, orbiting speed and orbital period. Birth RSO tracks are initialized in one or more CARs using the adaptive birth approach for labeled RFSs with appropriate birth probabilities using observations from the previous time step and CAR specific orbital parameters. The orbit tracks of RSOs from LEO to HEO can therefore theoretically be modeled using all captured observations. This concept is shown in Fig. 3.

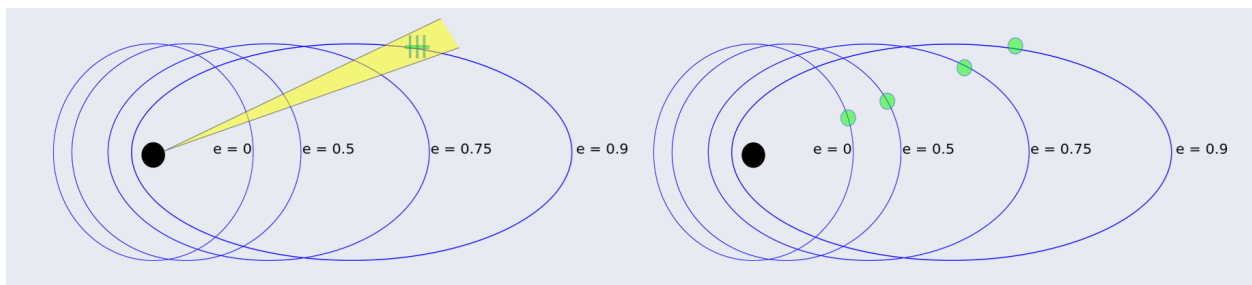


Fig. 3: (Left) Due to birth modelling with multiple CARs corresponding to multiple orbit possibilities, target tracks for the RSO in multiple orbits can be initialized. (Right) RSOs in multiple orbits can be tracked.

The dynamic motion of each RSO track is modeled using a JMS [12] such that each RSO track is allowed to switch between different motion models corresponding to different CARs. This allows an RSO track initialized in a particular CAR, with its corresponding orbital motion model, to switch to a different orbital motion model with a predefined transition probability. As a result, even with a limited number of target initializations, with increased measurement updates, its track is expected to converge to the correct CAR. This approach takes into account all possible track-to-measurement associations, new track initializations, possible switching of motion models, potential track deaths, miss-detections, and measurement clutter within a single Bayesian filtering framework. The highest weighted multi-target state hypothesis in the resulting truncated  $\delta$ -GLMB distribution represents the kinematic states, labels and the most probable CARs of the RSOs being tracked at any given time. The probabilities of detection and survival of an RSO are modeled by taking the current orbital motion model, estimated state of the RSO and the FOV of the telescope into account.

This article provides the details of the multi-PAR RSO tracker and provides preliminary results, showing how telescopic data can be suitably processed to provide the necessary input measurement data to the tracker.

## 2. MULTI-TARGET JUMP MARKOV $\delta$ -GLMB FILTER IMPLEMENTATION

This section presents the theory behind the RFS filtering algorithm that will be developed to solve the multi-target tracking problem in SSA. The section starts with an introduction to the theory of the  $\delta$ -GLMB filter [11][10], which is used as the base algorithm for the proposed solution.

Let the estimated state of a single RSO be represented by  $\mathbf{x} = [\rho, \alpha, \beta, \dot{\rho}, \dot{\alpha}, \dot{\beta}]^T$  and let the observation of an RSO be represented by  $\mathbf{z} = [\alpha, \beta]^T$ , where  $\alpha$  and  $\dot{\alpha}$  represent the right ascension and its rate of change,  $\beta$  and  $\dot{\beta}$  represent the declination and its rate of change and  $\rho$  and  $\dot{\rho}$  represent the estimated range and range rate of the RSO with respect to the telescope.

Let the time sequence of sets of observations acquired from a sequence of telescopic images be denoted by  $Z_{1:k} = [Z_1, Z_2, \dots, Z_k]$ , where  $Z_k = \{\mathbf{z}_{k,1}, \mathbf{z}_{k,2}, \dots, \mathbf{z}_{k,n_k}\}$  denotes the measurement detection set received at time  $k$ , where  $n_k$  denotes the number of detections. Let  $\mathbf{y}_{1:k} = [\mathbf{y}_1, \mathbf{y}_2, \dots, \mathbf{y}_k]^T$ , where  $\mathbf{y}_k$  denotes the pose of the telescope in the Earth Centered Inertial (ECI) coordinate frame at time  $k$  and assume that it is a known quantity without uncertainty.

### 2.1 The $\delta$ -GLMB Filter

This section describes the  $\delta$ -GLMB filter, which will be used to develop the RSO tracking algorithm. The  $\delta$ -GLMB filter models the birth targets as a multi-Bernoulli distribution and it propagates the multi-target state, which consists of both kinematic states and target identities.

To reduce the computational cost of the original  $\delta$ -GLMB filter, Vo. et al. proposed an efficient implementation of the  $\delta$ -GLMB filter in [9], with joint prediction/update and a Gibbs sampling based truncation approach, resulting in large computational savings. In this work we adopt this version of the filter as explained in the following sub-sections.

#### 2.1.1 Labeled RFS representation of the Multi-target state

Let the multi-target state be represented as a labeled RFS  $X_k = \{\hat{\mathbf{x}}_{k,1}, \hat{\mathbf{x}}_{k,2}, \dots, \hat{\mathbf{x}}_{k,m_k}\}$  where  $m_k$  denotes the number of estimated RSOs being tracked at time  $k$ . Each realization of an RSO  $\hat{\mathbf{x}} \in X$  is of the form  $\hat{\mathbf{x}} = (\mathbf{x}, l)$ , where  $\mathbf{x} \in \mathbb{X}$  is the kinematic state and  $l \in \mathbb{L}$  is a distinct label of the point  $\mathbf{x}$ . Distinct labels provide a method to distinguish between RSOs [10], [11].

Let the kinematic state space of multi-target state be denoted by  $\mathbb{X}$  and the discrete label space be denoted by  $\mathbb{L}$ . Further, let  $\mathcal{L} : \mathbb{X} \times \mathbb{L} \rightarrow \mathbb{L}$  be the projection from labeled RFSs to labels defined by  $\mathcal{L}(\mathbf{x}, l) = l$ . Let the Kronecker delta function for arbitrary arguments (such as vectors, sets or integers) be denoted by  $\delta_Y(X)$ , which takes the value of 1 only if  $X = Y$  and 0 otherwise. The indicator function  $1_X(Y)$  takes the value of 1 if  $Y \in X$  and 0 otherwise. Let  $\Delta(X) \triangleq \delta_{|X|}(|\mathcal{L}(X)|)$  denote the distinct label indicator, which takes the value of 1 if and only if the labeled set  $X$  has the same cardinality as its labels  $\mathcal{L}(X) = \{\mathcal{L}(\hat{\mathbf{x}}) : \hat{\mathbf{x}} \in X\}$  and 0 otherwise. Let  $\mathcal{F}(J)$  represent all finite subsets of a set  $J$ . The inner product of two continuous functions is denoted by  $\langle f, g \rangle \triangleq \int f(\mathbf{x})g(\mathbf{x})d\mathbf{x}$  and for a real valued function  $h(\mathbf{x})$ , the multi-object exponential is defined as  $h(\cdot)^X \triangleq \prod_{\mathbf{x} \in X} h(\mathbf{x})$ .

### 2.1.2 Observation Model

The measurement set received at time  $k$  contains both actual RSO observations and false alarms (measurement clutter). Let the RFS  $C_k$  denote the measurement clutter, then the measurements received at time  $k$  can be modelled by the RFS,

$$Z_k = C_k \cup \left[ \bigcup_{(\mathbf{x}_k, l_k) \in X_k} H_k(\mathbf{x}_k, l_k) \right], \quad (1)$$

where,  $H_k(\mathbf{x}_k, l_k)$  is a Bernoulli RFS representing the measurement corresponding to the observation of target  $(\mathbf{x}_k, l_k) \in X_k$ . Due to the limited FOV of the optical sensor,  $H_k(\mathbf{x}_k, l_k)$  can be a singleton of the form  $\{\mathbf{z}_k\}$  with probability of detection  $p_{\mathbf{D}}(\mathbf{x}_k, l_k | \mathbf{y}_k)$  or  $\emptyset$  with probability of  $1 - p_{\mathbf{D}}(\mathbf{x}_k, l_k | \mathbf{y}_k)$ . Note that the probability of detection is a function of target state and telescope pose. The measurement likelihood function conditioned on the detection of the target with state  $(\mathbf{x}_k, l_k)$  is given by  $g_k(\mathbf{z}_k | \mathbf{x}_k, l_k, \mathbf{y}_k)$ . Assuming that the measurements are conditionally independent of each other and the measurement clutter, the measurement likelihood function corresponding to the observations can be written as,

$$g(Z|X, \mathbf{y}) = \mathbf{e}^{-\langle \kappa, \mathbf{1} \rangle} \kappa^Z \sum_{\theta \in \Theta(\mathcal{L}(X))} [\psi_Z(\cdot; \theta)]^X, \quad (2)$$

where  $\kappa$  denotes the intensity of Poisson distributed measurement clutter. Further

$$\psi_Z(\mathbf{x}, l; \theta) = \begin{cases} \frac{p_{\mathbf{D}}(\mathbf{x}, l) g(\mathbf{z}_{\theta(l)} | \mathbf{x}, l, \mathbf{y})}{\kappa(\mathbf{z}_{\theta(l)})} & \text{if } \theta(l) > 0 \\ 1 - p_{\mathbf{D}}(\mathbf{x}, l) & \text{if } \theta(l) = 0, \end{cases} \quad (3)$$

where  $\theta$  is an association map of the form,  $\theta : \mathbb{L} \rightarrow \{0, 1, \dots, |Z|\}$  such that each distinct estimated target is associated with a distinct measurement (i.e.  $\theta(i) = \theta(i') > 0$  implies  $i = i'$ ). The set  $\Theta$  of all such association maps is called the association map space and a subset of association maps with domain  $\mathcal{S}$  is denoted by  $\Theta(\mathcal{S})$ . Note that, unlike traditional multi-target tracking applications, already estimated (and confirmed) targets, which exit the current telescopic FOV are retained in the multi-target state with probability of detection  $p_{\mathbf{D}}(\mathbf{x}, l) = 0$  during the measurement update step since they may reappear in the FOV of the telescope.

### 2.1.3 Multi-target transition model

New observations are captured in the FOV of the telescope and fused into the multi-target state. These new targets are modelled as the labeled RFS  $Q_k$  with the birth label space  $\mathbb{B}$ , and the corresponding birth density is assumed to be a labeled multi-Bernoulli density of the form,

$$f_B(Q_k) = \Delta(Q) [1 - r_B^{(\cdot)}]_{\mathbb{B} - \mathcal{L}(Q_k)} [1_{\mathbb{B}}(\cdot) r_B^{(\cdot)}]_{\mathcal{L}(Q_k)} [p_B]_{\mathcal{L}(Q_k)}^{\mathcal{L}(Q_k)}, \quad (4)$$

where a realization of  $r_B^{(\cdot)}$  is of the form  $r_B^{(l)} = r_B(\mathbf{x}, l)$  for any label  $l \in \mathbb{B} - \mathcal{L}(Q_k)$  and denotes the birth probability of the target with label  $l$  and  $p_B(\mathbf{x}, l)$  denotes its spatial distribution.

Furthermore, a portion of the already existing targets in the multi-target state appears in the current sensor FOV. Given the current multi-target state  $X$ , a target  $(\mathbf{x}_k, l_k) \in X$  may appear in the sensor FOV in the next time step with probability  $p_S(\mathbf{x}, l)$  and change its state to  $(\mathbf{x}_{k+1}, l_{k+1})$  with probability density  $f(\mathbf{x}_{k+1} | \mathbf{x}_k) \delta_{l_k}(l_{k+1})$ , or leave the sensor FOV with probability  $q_S(\mathbf{x}, l) = 1 - p_S(\mathbf{x}, l)$ . It is important to note that unlike traditional multi-target tracking applications, in RSO tracking, targets follow particular motion models, as they orbit the earth and may reappear in the telescope's FOV at a later time. In addition, the label of a target is preserved during the state transition. Assuming that the multi-target state is represented by  $X$ , the set of surviving targets in the next time step is modelled as a labeled multi-Bernoulli (LMB) RFS  $W$  with parameter set  $\{(p_S(\mathbf{x}, l), f(\cdot | \mathbf{x}) \delta_l(\cdot)) : (\mathbf{x}, l) \in X\}$ . The state transition is modelled as a LMB distribution given by,

$$f_S(W|X) = \Delta(W) \Delta(X) 1_{\mathcal{L}(X)}(\mathcal{L}(W)) [\Phi(W; \cdot)]^X, \quad (5)$$

where,

$$\Phi(W; \mathbf{x}_{k+1}, l_{k+1}) = \sum_{(\mathbf{x}_{k+1}, l_{k+1}) \in W} \delta_{l_k}(l_{k+1}) p_S(\mathbf{x}_k, l_k) \delta_{\mathbf{x}_k}(\mathbf{x}_{k+1}) + [1 - 1_{\mathcal{L}(W)}(l_k)] q_S(\mathbf{x}_k, l_k). \quad (6)$$

The newly appearing (birth) targets are assumed to be independent of the already existing targets in the multi-target state. Therefore, it can be shown that the probability density of the predicted multi-target state  $X_{k+1}$ , conditioned on the current state  $X_k$ , can be written as a product of the birth and transition densities of the surviving targets [11],

$$f(X_{k+1}|X_k) = f_S(X_{k+1} \cap (\mathbb{X} \times \mathbb{L})|X_k) \times f_B(X_{k+1} - (\mathbb{X} \times \mathbb{L})). \quad (7)$$

Note that, the estimated targets that exit the current sensor FOV should remain in the multi-target state and be modelled with probability of survival  $p_S(\mathbf{x}, l) = 1$  during the prediction step.

### 2.1.4 The Joint prediction/update method

To propagate the multi-target state in time, the recently proposed efficient  $\delta$ -GLMB filter [9] is adopted. Let the multi-target posterior at time  $k$ ,  $p(X_k|Z_{1:k}, \mathbf{y}_{0:k})$  be abbreviated as  $p(X)$  and let the measurement updated multi-target posterior at time  $k+1$  be abbreviated as  $p(X_+|Z_+)$ . Assume that  $p(X)$  at time  $k$  is given by a  $\delta$ -GLMB distribution of the following form,

$$p(X) = \Delta(X) \sum_{(I, \xi) \in \mathcal{F}(\mathbb{L}) \times \Xi} \omega^{(I, \xi)} \delta_I(\mathcal{L}(X)) [p^{(\xi)}]^X, \quad (8)$$

where  $I \in \mathcal{F}(\mathbb{L})$  represents a set of target labels and  $\xi \in \Xi$  represents a history of association maps up to time  $k$  and denoted by  $\xi = (\theta_1, \dots, \theta_k)$ . The pair  $(I, \xi)$  represents the hypothesis that the set of targets  $I$  has history  $\xi$  of association maps and the weight  $\omega^{(I, \xi)}$  represents the probability of the hypothesis  $(I, \xi)$  and  $p^{(\xi)}(\mathbf{x}, l)$  represents the probability density of the kinematic state of the target with label  $l$  and the association map history  $\xi$ .

Assume that the birth targets (newly appearing targets) and the surviving targets in the limited sensor FOV assume labeled multi-Bernoulli distributions. Let  $\mathbb{B}_+$  denote the label space of newly appearing targets in the FOV at time  $k+1$ . Then, adopting the joint prediction/update approach proposed in [9], the measurement updated multi-target posterior  $p(X_+|Z_+)$  can be written as,

$$p(X_+|Z_+) \propto \Delta(X_+) \sum_{I, \xi, I_+, \theta_+} \bar{\omega}_{Z_+}^{(I, \xi, I_+, \theta_+)} \delta_{I_+}(\mathcal{L}(X_+)) [p_{Z_+}^{(\xi, \theta_+)}]^{X_+}, \quad (9)$$

where  $\mathbb{L}_+ = \mathbb{L} \cup \mathbb{B}_+$ ,  $\mathcal{I}_+ \in \mathcal{F}(\mathbb{L}_+)$ ,  $\theta_+ \in \Theta_+$ .  $\Theta_+$  denotes the association map space at time  $k+1$ , and

$$\bar{\omega}_{Z_+}^{(I, \xi, I_+, \theta_+)} = \omega^{(I, \xi)} \omega_{Z_+}^{(I, \xi, I_+, \theta_+)}, \quad (10)$$

$$w_{Z_+}^{(I, \xi, I_+, \theta_+)} = \mathbf{1}_{\Theta_+(I_+)}(\theta_+) [1 - \bar{P}_S^{(\xi)}]^{I-I_+} [\bar{P}_S]^{I \cap I_+} [1 - r_{B,+}^{(\cdot)}]^{(\mathbb{B}_+ - I_+)} r_{B,+}^{(\mathbb{B}_+ \cap I_+)} [\bar{\psi}_{Z_+}^{(\xi, \theta_+)}]^{I_+}, \quad (11)$$

$$\bar{P}_S^{(\xi)}(l) = \langle p^{(\xi)}(\cdot, l), p_S(\cdot, l) \rangle, \quad (12)$$

$$\bar{\psi}_{Z_+}^{(\xi, \theta_+)}(l_+) = \langle \bar{p}_+^{(\xi)}(\cdot, l_+), \psi_{Z_+}^{(\theta_+(l_+))}(\cdot, l_+) \rangle, \quad (13)$$

where  $\psi_{Z_+}^{(\theta_+(l_+))}(\mathbf{x}_+, l_+) = \psi_{Z_+}(\mathbf{x}_+, l_+; \theta_+)$  (see (3)). Further

$$\bar{p}_+^{(\xi)}(\mathbf{x}_+, l_+) = \mathbf{1}_{\mathbb{L}}(l_+) \times \frac{\langle p_S(\cdot, l_+) \delta_{(\cdot)}(\mathbf{x}_+), p^{(\xi)}(\cdot, l_+) \rangle}{\bar{P}_S^{(\xi)}(l_+)} + \mathbf{1}_{\mathbb{B}_+}(l_+) p_{B,+}(\mathbf{x}_+, l_+), \quad (14)$$

$$p_{Z_+}^{(\xi, \theta_+)}(\mathbf{x}_+, l_+) = \frac{\bar{p}_+^{(\xi)}(\mathbf{x}_+, l_+) \psi_{Z_+}^{(\theta_+(l_+))}(\mathbf{x}_+, l_+)}{\bar{\psi}_{Z_+}^{(\xi, \theta_+)}(l_+)} \quad (15)$$

where the notation  $+$  has been used to abbreviate the symbols at time  $k+1$  and  $r_{B,+}^{(l_+)}$  denotes the probability of birth of the target  $l_+$ . The spatial distribution of each birth target,  $p_{B,+}(\mathbf{x}_+, l_+)$ , is modelled as a Gaussian and hence the resultant  $\delta$ -GLMB filter follows a Gaussian mixture representation, where the spatial distribution of each target with label  $l$  in each hypothesis results in a mixture of Gaussian distributions.

The idea behind the joint prediction/update approach using the Gibbs sampler is to generate a smaller number of highly probable hypotheses using existing hypotheses, probability of detection and probability of survival of targets and the set of received measurements at time  $k+1$ . This prevents the generation of insignificant and contradicting hypotheses and drastically reduces the computational complexity compared to the traditional prediction/update based  $\delta$ -GLMB filter implementation [10] yielding a computationally efficient alternative for real-time implementations.

## 2.2 JMS Modelling in the $\delta$ -GLMB Filter

The multi-target state is represented as a labeled RFS  $X_k = \{\mathbf{x}'_{k,1}, \mathbf{x}'_{k,2}, \dots, \mathbf{x}'_{k,m_k}\}$  to cater for RSOs with multiple motion models, where each realization of an RSO  $\mathbf{x}' \in X$  is augmented with a motion model as  $\mathbf{x}' = (\mathbf{x}, o, l)$ , where  $o \in \mathbb{O}$  denotes the motion model, and  $\mathbb{O}$  denotes the discrete space of all possible motion models.

The multi-target posterior with multiple motion models is given by,

$$p(X) = \Delta(X) \sum_{(I,\xi) \in \mathcal{F}(\mathbb{L}) \times \Xi} \omega^{(I,\xi)} \delta_I(\mathcal{L}(X)) [p^{(\xi)}]^X, \quad (16)$$

where  $p^{(\xi)}(\mathbf{x}, o, l)$  represents the probability density function of the kinematic state of the target with motion model  $o$ , label  $l$  and the association map history  $\xi$ . Then, using the joint prediction/update approach [9], the measurement updated multi-target posterior with multiple motion models is given by

$$p(X_+ | Z_+) \propto \Delta(X_+) \sum_{I, \xi, l_+, \theta_+} \bar{\omega}_{Z_+}^{(I, \xi, l_+, \theta_+)} \times \delta_{I_+}(\mathcal{L}(X_+)) [p_{Z_+}^{(\xi, \theta_+)}]^{X_+}, \quad (17)$$

where,

$$\bar{\omega}_{Z_+}^{(I, \xi, l_+, \theta_+)} = \omega^{(I, \xi)} \omega_{Z_+}^{(I, \xi, l_+, \theta_+)}, \quad (18)$$

$$w_{Z_+}^{(I, \xi, l_+, \theta_+)} = \mathbf{1}_{\Theta_+(l_+)}(\theta_+) [1 - \bar{P}_S^{(\xi)}]^{l-l_+} [\bar{P}_S]^{l \cap l_+} [1 - r_{B,+}^{(\cdot)}]^{(\mathbb{B}_+ - l_+)} r_{B,+}^{(\mathbb{B}_+ \cap l_+)} [\bar{\psi}_{Z_+}^{(\xi, \theta_+)}]^{l_+}, \quad (19)$$

where  $r_{B,+}^{(l_+, o_+)}$  denotes the probability of birth of the target with  $l_+$  and motion model  $o_+$ . Further

$$\bar{P}_S^{(\xi)}(l) = \sum_{o \in \mathbb{O}} \langle p^{(\xi)}(\cdot, o, l), p_S(\cdot, o, l) \rangle, \quad (20)$$

$$\bar{\psi}_{Z_+}^{(\xi, \theta_+)}(l_+) = \sum_{o_+ \in \mathbb{O}} \langle \bar{p}_+^{(\xi)}(\cdot, o_+, l_+), \psi_{Z_+}^{(\theta_+(l_+))}(\cdot, o_+, l_+) \rangle, \quad (21)$$

where  $\psi_{Z_+}^{(\theta_+(l_+))}(\mathbf{x}_+, o_+, l_+) = \psi_{Z_+}(\mathbf{x}_+, o_+, l_+; \theta_+)$ , which is given by

$$\psi_{Z_+}(\mathbf{x}, o, l; \theta) = \begin{cases} \frac{p_{\mathbf{D}}(\mathbf{x}, o, l) g(\mathbf{z}_{\theta(l)} | \mathbf{x}, o, l, \mathbf{y})}{\kappa(\mathbf{z}_{\theta(l)})} & \text{if } \theta(l) > 0 \\ 1 - p_{\mathbf{D}}(\mathbf{x}, o, l) & \text{if } \theta(l) = 0 \end{cases} \quad (22)$$

and,

$$\bar{p}_+^{(\xi)}(\mathbf{x}_+, o_+, l_+) = \mathbf{1}_{\mathbb{L}}(l_+) \sum_{o \in \mathbb{O}} \frac{\langle p_S(\cdot, o, l_+) f(\mathbf{x}_+, o_+, l_+ | \mathbf{x}, o, l), p^{(\xi)}(\cdot, o, l_+) \rangle}{\bar{P}_S^{(\xi)}(l_+)} + \mathbf{1}_{\mathbb{B}_+}(l_+) p_{B,+}(\mathbf{x}_+, o_+, l_+), \quad (23)$$

$$p_{Z_+}^{(\xi, \theta_+)}(\mathbf{x}_+, o_+, l_+) = \frac{\bar{p}_+^{(\xi)}(\mathbf{x}_+, o_+, l_+) \psi_{Z_+}^{(\theta_+(l_+))}(\mathbf{x}_+, o_+, l_+)}{\bar{\psi}_{Z_+}^{(\xi, \theta_+)}(l_+)} \quad (24)$$

where,  $f(\mathbf{x}_+, o_+, l_+ | \mathbf{x}, o, l)$  is the state transition density given by

$$f(\mathbf{x}_+, o_+, l_+ | \mathbf{x}, o, l) = f(\mathbf{x}_+ | \mathbf{x}, o) \delta_{(l)}(l_+) t_{k|k-1}(o_+ | o). \quad (25)$$

$t_{k|k-1}(o_+ | o)$  denotes the transition probability from motion model  $o$  to  $o_+$ . The spatial distribution of each birth target,  $p_{B,+}(\mathbf{x}_+, o_+, l_+)$ , is modelled as a Gaussian and hence the resultant  $\delta$ -GLMB filter follows a Gaussian mixture representation similar to the non-maneuvering case. A summary of the  $\delta$ -GLMB implementation is shown in Figure 4.

## 3. IMPLEMENTATION & PRELIMINARY RESULTS

This section provides the telescopic data processing details necessary to provide suitable measurement information to the JMS  $\delta$ -GLMB tracker. In particular, the preliminary post processing results of a sequence of telescopic images of the NORAD satellite 25853, acquired from a wide FOV optical telescope with sidereal tracking mode, are presented. A pair of right ascension and declination values corresponding to the two ends of each streak are found by streak extraction and plate solving algorithms. Fig. 5 shows the flow diagram of the steps required to produce measurements from the telescopic images to be used as inputs to the proposed RFS based multi-target tracking algorithm.

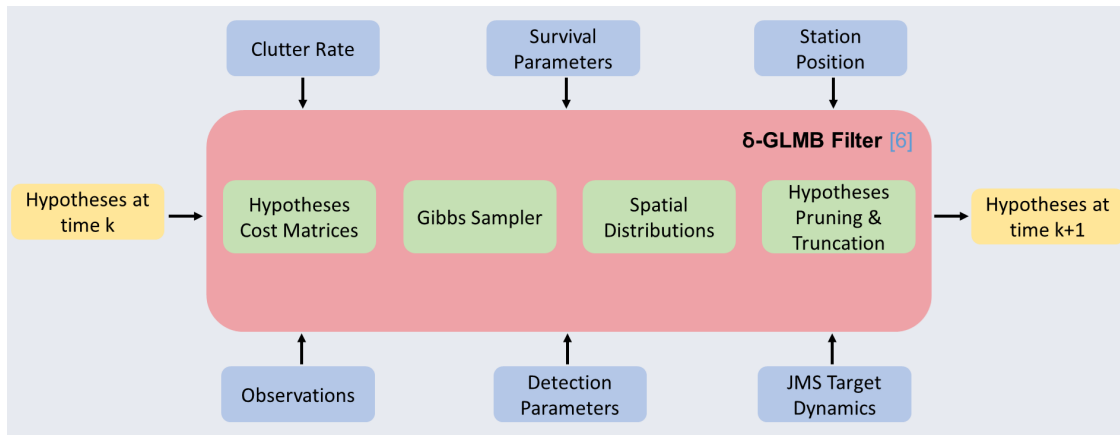


Fig. 4: Block diagram of the JMS  $\delta$ -GLMB RSO tracker.

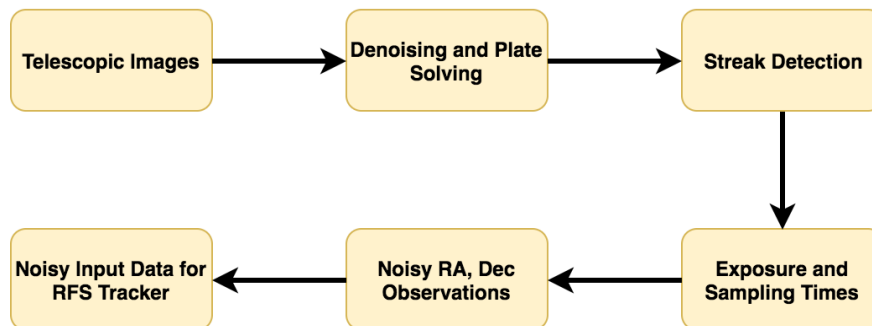


Fig. 5: Processing telescopic images to produce right ascension (RA) and declination (Dec) measurements for the RSO tracker.

### 3.1 Streak Detection

Sidereal tracking of RSOs may produce streaks in the telescopic images depending on their speed and distance from the earth. In order to track such RSOs, it is required to process and extract the information contained in such streaks. In this work we extract the pixel positions of both ends of each streak and the corresponding RA and Dec pairs are generated using the plate solving results. For offline processing, the travel direction of a streak is determined by comparing either the RA or Dec values of two consecutive images with known timestamps.

In this work, the software ASTRiDE [5] is adopted to detect the streaks from the telescopic images. The algorithm proceeds as follows:

- Background removal: Background is removed using the same procedure described in [1].
- Contour map generation: Obtains closed contours of detected RSOs segmented by a threshold over the image without the background.
- Streak Determination: Removes all detections that are not streak-like, based on the morphological parameters such as shape factor, radius deviation and area. Shape factor indicates the similarity between an object to a circle. A value of 1.0 indicates a circular shape and a value of near 0 indicates a line-like streak.
- Streak Fusion: The streaks that are close to each other with similar gradients are fused, while streaks with distinctive gradients form multiple streaks.

A flow diagram summarizing the processing steps of the ASTRiDE software is shown in Fig.6 and an image containing a streak, and its detection are shown in the left and right images of Fig. 7 respectively.

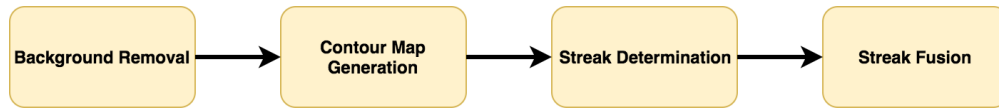


Fig. 6: Flow diagram of the open source ASTRiDE streak detector.

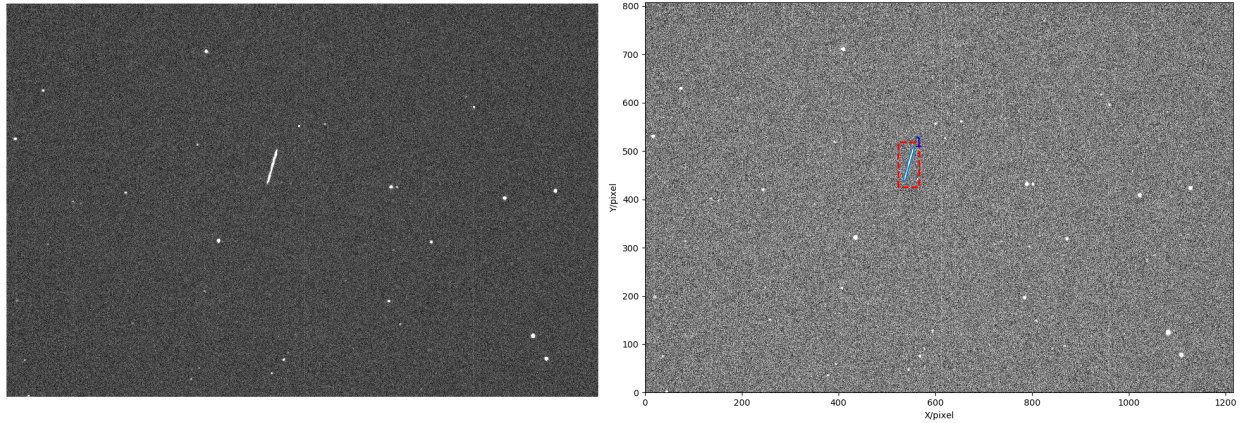


Fig. 7: Streak detection results from the sidereal tracking of NORAD Satellite 25853.

### 3.2 Astrometric Calibration (Plate Solving)

Plate solving (Fig. 8) is performed in order to generate the required information to map an input pixel of an astronomical image to celestial coordinates (RA and Dec). In this work, plate solving was performed using the Astrometry.net

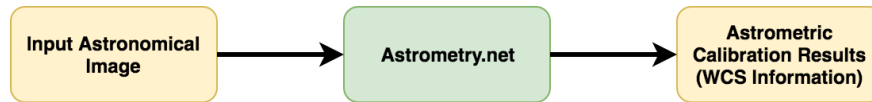


Fig. 8: The plate solving process using Astrometry.net.

software [6], and the main steps involved are summarized in Fig.9. The resultant world coordinate system (WCS) information [2] is used to convert a pixel value in the input image into corresponding celestial coordinates and used as inputs in the RFS based tracking algorithms.

## 4. CONCLUSIONS & FUTURE WORK

As a feasibility study for providing useful measurement data for the proposed JMS  $\delta$ -GLMB RSO tracker, an optical telescopic image sequence taken from the sidereal tracking of a satellite was obtained from the Mitre Corporation. Astrometric calibration was performed on the image sequence using the Astrometry.net software to convert pixels into celestial coordinates (right ascension and declination). Satellite streaks were detected from the ASTRiDE software and the pixels that corresponds to both ends of streaks were converted into celestial coordinates. These coordinate pairs will be used as the inputs to the JMS  $\delta$ -GLMB RSO tracking algorithm in future work.

The proposed multiple Probabilistic Admissible Region (PAR) approach to initialize the orbits of RSOs will be further investigated and corresponding birth target approaches will be devised for the  $\delta$ -GLMB filter.

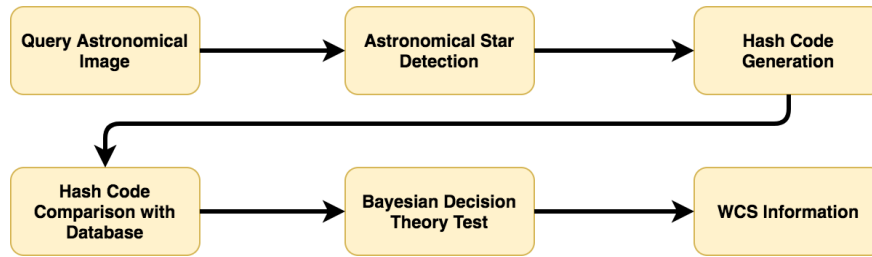


Fig. 9: The processing steps of the Astrometry.net software. The query image is hashed [8] and compared to an existing database (USNO-B Catalog).

## ACKNOWLEDGMENTS

This material is based upon work supported by the US Air Force Office of Scientific Research under award number FA9550-17-1-0386. We would also like to thank Prof. Francis Chun from USAFA, USA and Dr. José Luis E. Nilo Castellon from Universidad de La Serena, Chile for providing telescopic images from the Falcon Telescope Network (FTN). Further telescopic images were obtained with thanks from Mr. Tim McLaughlin, Mitre Corporation, USA.

## 5. REFERENCES

- [1] E. Bertin and S. Arnouts. SExtractor: Software for source extraction. *Astronomy and Astrophysics Supplement Series*, 117(2):393–404, December 1996.
- [2] M.R. Calabretta and E.W. Greisen. Representations of celestial coordinates in FITS. *Astron. Astrophys.*, 395:1077, 2002.
- [3] I. Hussein, C. Roscoe, M. Wilkins, and P. Schumacher. Probabilistic Admissible Region for Short-Arc Angles-Only Observations. In *Proceedings of the Advanced Maui Optical and Space Surveillance Technologies Conference*, September 2014.
- [4] B.A. Jones, B.-T. Vo, and B.-N. Vo. Generalized Labeled Multi-Bernoulli Space-Object Tracking with Joint Prediction and Update. In *AIAA/AAS Astrodynamics Specialist Conference*, pages 1177–1194, Long Beach, CA, USA, September 2016.
- [5] D.-W. Kim, Y.-I. Byun, S.-Y. Kim, Y.-W. Kang, W. Han, H.-K. Moon, and A.-S. Yim. Automated streak detection for high velocity objects: Test with ystar-neopap images. *Journal of Astronomy and Space Sciences*, 22, 2005.
- [6] D. Lang, D. W. Hogg, K. Mierle, M. Blanton, and S. Roweis. Astrometry.net: Blind astrometric calibration of arbitrary astronomical images. *arXiv:0910.2233*, 137:1782–2800, 2010.
- [7] A. Milani, G.F. Gronchi, M. Vitturi, and Z Knežević. Orbit determination with very short arcs. I admissible regions. In *Celestial Mechanics and Dynamical Astronomy*, pages 59–87. Pisa, Italy, December 2004.
- [8] A. Swaminathan, Y. Mao, and M. Wu. Robust and secure image hashing. *IEEE Trans. Information Forensics and Security*, 1(2):215–230, June 2006.
- [9] B.-N. Vo, B.-T. Vo, and H.G. Hoang. An Efficient Implementation of the Generalized Labeled Multi-Bernoulli Filter. *IEEE Transactions on Signal Processing*, 65(8):1975–1987, June 2018.
- [10] B.-N. Vo, B.-T. Vo, and D. Phung. Labeled Random Finite Sets and the Bayes Multi-Target Tracking Filter. *IEEE Transactions on Signal Processing*, 62:6554–6567, December 2014.
- [11] B.-T. Vo and B.-N. Vo. Labeled random finite sets and multi-object conjugate priors. *IEEE Transactions on Signal Processing*, 61(13):3460–3475, June 2013.
- [12] W. Yi, M. Jiang, and R. Hoseinnezhad. The Multiple Model Vo-Vo Filter. *IEEE Transactions on Aerospace and Electronic Systems*, 53(2):1045–1054, April 2017.